Al-Azhar Engineering 16th International Conference

Vol. 19, No. 72, July 2024, 234 - 249

LOAD FREQUENCY CONTROL OPTIMIZATION USING MGO-BASED PIDF IN THREE-AREA SYSTEMS WITH ENERGY STORAGE

Abdulslam A. Aloukili[1]*, Tarek M. Nasser[2], Mohammed A. Mehanna[2]

[1] Electrical Engineering Department, Faculty of Engineering, University of Dernah, Dernah, Libya

[2]Electrical Engineering Department, Faculty of Engineering, Al-Azhar University, Cairo, Egypt

*Corresponding Author: a.alaokali@uod.edu.ly

Citation:

A.A. Aloukili, T.M. Nasser and M.A. Mehanna, "load frequency control optimization using mgo-based pidf in three-area systems with energy storage" Journal of Al-Azhar University Engineering Sector, vol. 19, pp. 234 - 249, 2024.

Received: 23 November 2023

Revised: 04 January 2024

Accepted: 20 January 2024

DoI:10.21608/auej.2024.250791.1483

ABSTRACT

Maintaining the stability and reliability of power systems is a key function of load frequency control (LFC). However, issues such as load variations, network challenges, and introducing renewable energy sources complicate this task. Consequently, devising an efficient controller for LFC becomes a complex optimization issue. In this paper, we propose a distinctive controller for LFC built on a proportional-integral-derivative (PID) controller and a derivative filter (PIDF). To find the optimum parameters of PIDF controllers, use Mountain Gazelle Optimizer (MGO), an algorithm that draws inspiration from the behavior of mountain gazelles. The performance of this controller is contrasted with that of another PIDF controller that leverages the Harmony Search (HS) algorithm. The controllers are evaluated using a three-area non-reheat thermal system, both with and without storage systems like superconducting magnetic energy storage (SMES) and battery energy storage (BES). The Integral Time Absolute Error (ITAE) serves as the objective function for the assessment of these controllers. The MGO-based PIDF controller with Energy Storage (ES) works better than the HS-based PIDF controller with and without ES, as well as the MGO-based PIDF controller without ES, when ITAE, frequency deviation, and tie-line power deviation are taken into account. Furthermore, the MGO-based PIDF controller exhibits superior robustness and noise immunity compared to the others. In conclusion, the controller proposed in this paper presents a potential solution for LFC in contemporary power systems.

KEYWORDS: load frequency control, Mountain Gazelle Optimizer, Energy Storage, Integral Time Absolute Error

تحسين التحكم في تردد الحمل باستخدام الحاكم التفاضلي التناسبي التكاملي معتمدا على تقنية غزل الجبل للتحسين لنظام مكون من ثلاث مناطق مع انظمة تخزين الطاقة

عبدالسلام عارف العوكلي [1]*، طارق محمود ناصر[2]، محمد احمد مهنى [2]

[1]قسم االهندسة الكهربائية ، كلية الهندسة، جامعة درنة، مدينة درنة. ليبيا

[2]قسم االهندسة الكهربية، كلية الهندسة، جامعة الأزهر، مدينة نصر، 11884، القاهرة، مصر.

البريد الاليكتروني للباحث الرئيسي*: a.alaokali@uod.edu.ly

الملخص

يشكل الحفاظ على استقرار وموثوقية نظم الطاقة إحدى الوظائف الرئيسية لمتحكم تردد الحمل . ومع ذلك، فإن تباين الأحمال، والتحديات التي تواجهها الشبكات نتيجة توسعها وإدخال مصادر الطاقة المتجددة تؤدي إلى تعقيد هذه المهمة. وبناء على ذلك، يصبح استحداث متحكم قوي في التردد لمقابلة هذه التغير المفاجي في الاحمال مهم جدا . في هذه الورقة، نقترح متحكماً فريداً لتردد الحمل التي تستند إلى الحاكم التناسبي التفاضلي المشهورمع مرشح للحاكم التفاضلي. ويضبط هذا المتحكم باستخدام خوارزمية مستوحاة من سلوك غزال الجبال، تستخدم في ضبط بارامترات المتحكم التفاضلي التناسبي التكاملي. ويتم مقارنة هذا المتحكم مع متحكم اخر يتم ضبطة بخوارزمية البحث عن الانسجام . ويجري تقييم المتحكمين باستخدام شبكه كهربائية مكونه من ثلاث مناطق، مع و بدون انظمة التخزين، مثل نظم التخزين مثل تخزين الطاقة المغنطيسية ومخازن طاقة البطاريات . ويعمل الخطأ المطلق لوقت التكامل كوظيفة موضوعية لتقييم هذه الضوابط. وعند النظر في انحراف التردد وانحراف القدرة عن طريق خطوط الربط، فإن المتحكم الذي يستند إلى مع تخزين الطاقة، ، يتفوق في أداء المتحكم القائم على مع أو بدون انطمه تخزين الطاقة ، وكذلك المتحكم القائم على بدون تخزين الطاقة. علاوة على ذلك، يظهر المتحكم المقترح تحملًا فائقًا ومناعة للضوضاء مقارنة بالآخرين. وفي الختام، يقدم المتحكم المقترح في هذه الورقة حلًا محتملاً للتحكم في تردد الحمل في أنظمة الطاقة الحديثة.

الكلمات الرئيسية: التحكم في تردد التحميل، محسن غزال الجبل، تخزين الطاقة، الخطأ المطلق الوقت الكلي.

1. INTRODUCTION

In the evolution of modern electrical power networks, there has been a growing emphasis on renewable energy sources and energy storage in recent years. The incorporation of different energy sources has created new issues in terms of balancing output and consumption. To overcome these challenges, load frequency control is more important than ever. Load frequency control is critical in modern power systems because it keeps frequency and voltage steady amid rapid load changes. This study covers the role of load frequency management in modern electrical power networks, especially with the incorporation of energy storage, to ensure system stability in the face of unexpected load shifts.

Load-frequency control (LFC) is essential to ensuring power system stability. Various types of research have been offered, as well as several case studies, to create a successful LFC system. Fuzzy logic, neural networks, evolutionary algorithms, and adaptive control are examples of techniques for improving the efficacy and robustness of LFC. These strategies can deal with the uncertainties, nonlinearities, and disturbances that affect frequency control and system dynamics [1-3]. Here are some examples of advanced control techniques: In contrast to mathematical models, fuzzy logic control (FLC) is an approach for constructing controllers based on linguistic norms and fuzzy sets. FLC is capable of handling imperfect and insufficient data while still providing smooth and flexible control actions [1]. Neural network control (NNC) is an approach for developing controllers based on artificial neural networks, which are computational models that imitate biological neurons' learning capacity. NNCs can learn from data, adapt to changing conditions, and perform nonlinear and optimal control actions [1]. The genetic algorithm (GA) is a method for optimizing controller parameters based on natural selection and evolution concepts. GA is capable of searching for optimal solutions in a broad, complex space and producing global, robust optimization results [2]. AC is a method of building controllers that can change their parameters or structure depending on the system's states or outputs. AC is capable of dealing with parameter discrepancies and disruptions. These strategies can be used to improve LFC in a variety of power systems, including interconnected multi-area power systems, wind-thermal-hydro power systems, intelligent grids with demand

response, and renewable energy sources. These strategies can help improve the frequency response, damping ratio, settling time, overshoot, and steady-state error of an LFC [3-4].

The microgrid is a networked power generation system made up of several interconnected generators. Non-reheat turbines, thermal turbines, gas turbines, nuclear reactors, wind turbines, PVs, and other generators may be found in any location. These generators can all be linked in one or more places. In the power system, strong generation control is always necessary, especially in utility systems with a significant penetration of renewable energy sources (RES). Increasing the percentage of renewable energy in a power system lessens its inertia and resistance to unexpected load shifts or other disturbances. [4-7].

Numerous academics have offered a variety of difficulties and solutions for maintaining load frequency management. To improve LFC in three areas, [8] suggested an effective active disturbance rejection control. In [5], the authors investigated the influence of storage systems in three area systems with combined RES and AVR control. The authors presented the innovative technique GA-PSO to improve the PID controller for a more resilient three-area system [9]. A fractional-order PID controller was utilized in [10] to improve LFC in three-area systems. The authors in [11] used an artificial neural network to optimize a four-area interconnected system. Furthermore, the authors presented a FOPID controller to improve a four-area RES-integrated system [12]. PSO is combined with a fuzzy logic controller in [13] to optimize PID controller parameters. The authors of [14] implemented a firefly algorithm to improve load frequency control in the fore area system. In [15], an ANFIS controller was used to enhance the LFC in conjunction with the SMES-TCPS.

To improve LFC on the multi-area system, [16] used a PI-PID cascade controller based on the Flower Pollination algorithm. The authors in [17] created a method for improving the PID on LFC using ANFIS. Deep learning approaches were also employed to improve generation control and reduce frequency deviation [18]

This study will utilize a three-area non-reheating system that incorporates a PID controller with a derivative filter. The controller will be tuned using optimization techniques such as Mountain Gazelle Optimizer and harmony search algorithm. Energy storage systems such as SMEs and BES will be used to support the non-reheating. The first section of this work introduces the study, while the second section describes and models the system. The third section discusses the study's control strategy, and the fourth section presents findings and discussions. The last section brings this work to a close.

2. System description and modeling

2.1 System description

In this work, a three-area non-reheat thermal system is adopted. Each area is equipped with a single generator, turbine, and governor, as well as loads and energy storage systems. When the load increases or a malfunction develops in the system that causes the frequency to decelerate or accelerate, the controller must modify the system settings to restore stability. Each of the three area of the system illustrated in Figure 1 Simple sketch contains one turbine, one governor, and one generator. Areas one, two, and three each have a rating of 2000MW [19-22]. To boost the system's performance, energy storage devices are also added.

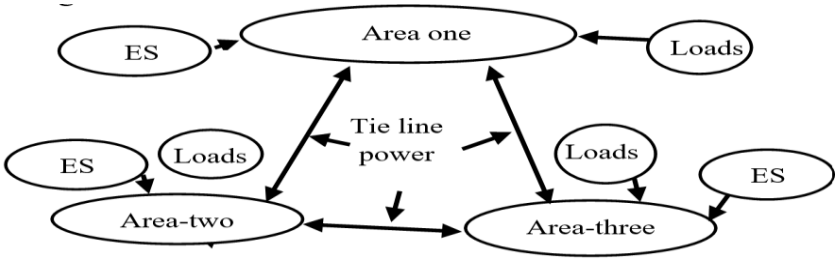

Fig 1: Simple sketch three-area non-reheat system diagram with energy storge system

The power rating for each area is also 2000 MW. The inertia for each generator in each area is 5 pu.MW s, which represents the amount of kinetic energy stored in the rotating mass of the generator and is used to measure the ability of the generator to resist changes in system frequency. The tie-line maximum power sharing across areas is 200 MW. For each location, the frequency base factor B is 0.425. The synchronization coefficients between areas are T12, T23, and T31. For each area, the LFC Participation Factor is equal to 1. Kpsi is the power system's gain. Each load and generation block, as shown in Figure 2, represents a first-order equation. There are also first-order equations characterizing the governors and turbines as demonstrate before in [23].

Table 1: Three area system parameters

Area	1	2	3	Units
Speed regulation	R=2.4	R=2.4	R=2.4	Hz/ PU MW
Tie-line max	200	200	200	MW
Base power	2000	2000	2000	MW
Governor time constant	T_g=0.08	T_g=0.08	T_g=0.08	second
Turbine time constant	T_t=0.3	T_t=0.3	T_t=0.3	second
K_{psi}	120	120	120	Non
β	0.425	0.425	0.425	Hz/MW
Time constant Tips	20	20	20	second
a	-1	-1	-1	Non
T_{12}=T_{23}=T_{31}	.08674	.08674	.08674	PU MW/Hz

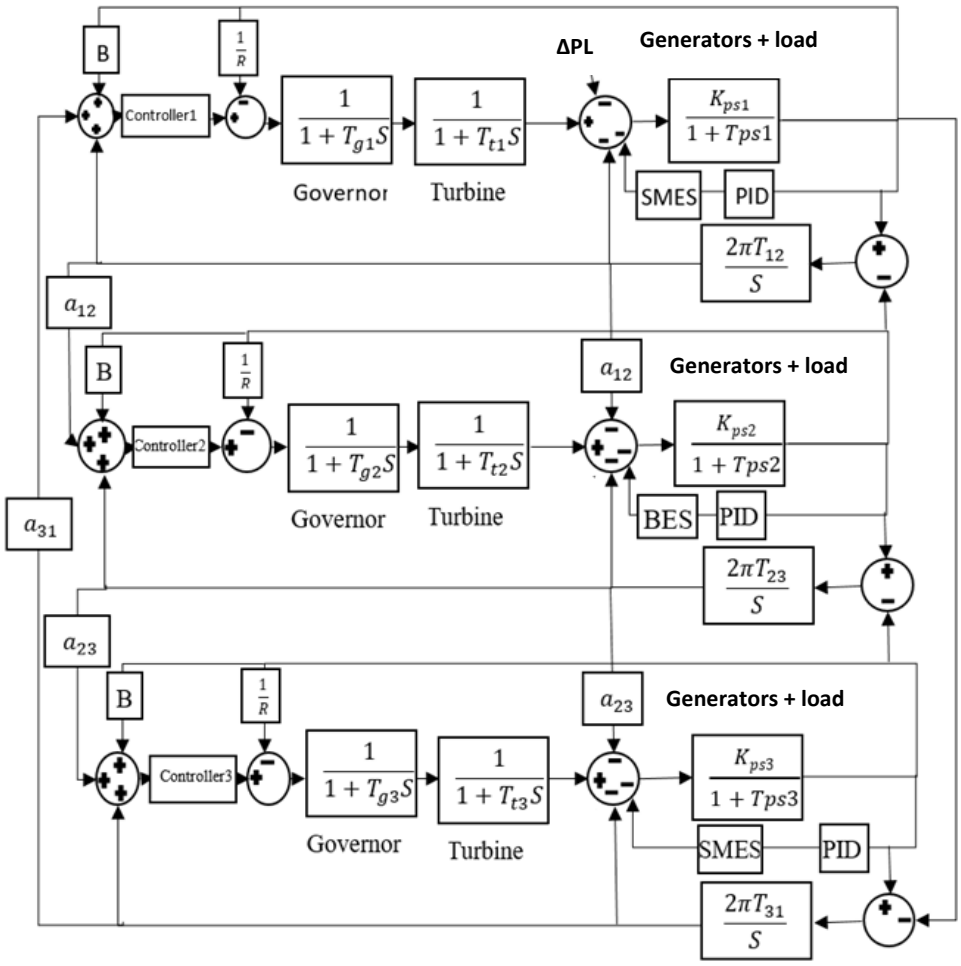

Fig.2: Block digram for three-area non-reheat system that incorporates storge energy

2.2 Problem formulation

The purpose of this article is to increase system stability, reduce overshoot, undershoot, and settling time by determining the appropriate controller parameters. The objective function utilized in this article is ITAE (integral time absolute error), which has been proven in [24] to be more effective than other approaches. ITAE minimizes the area control error (ACE) in each area, which is a function of the frequency deviation in the area Δf_i, where *i* is the number of area and the power tie-line $\Delta P_{tie\text{-}ij}$ between areas, such as area one and two. The objective function is defined in Equations (1-4) below. After 500 iterations, artificial intelligence (AI) will identify the ideal PID controller parameters. Three optimization approaches, MGO [25], and HSA [26], are employed to improve system performance. They are used to discover the best PID controller parameters.

$$\text{ITAE}=\int_0^\infty t|ACE_1 + ACE_2 + ACE_3|\, dt \quad \text{Eq.1}$$

Where

$$ACE_1= \Delta f_1+\Delta P_{tie\ 12}+ \Delta P_{tie\ 31} \quad \text{Eq.2}$$

$$ACE_2= \Delta f_2+\Delta P_{tie\ 23}+ \Delta P_{tie\ 12} \quad \text{Eq.3}$$

$$ACE_3= \Delta f_3+\Delta P_{tie\ 23}+ \Delta P_{tie\ 31} \quad \text{Eq.4}$$

3. Modeling of energy storage systems

SMES model

Superconducting magnetic energy storage (SMES) is a type of energy storage that stores energy by using the magnetic field produced by a superconducting coil. When an electric current flows through the coil, high-temperature superconductors generate a tremendous magnetic field. The stored energy can then be released by reversing the current flow, allowing for a large amount of energy to be discharged quickly. Power grid stabilization, peak shaving, and load leveling are all common uses for SMES systems [5,7]. Power (P) and magnetic energy (E) calculations are as follows:

$$E = \int P\,dt = \int VI\,dt \quad \text{Eq.5}$$

$$E = L\int i.\frac{di}{dt}\,dt = \frac{1}{2}\,LI^2 \quad \text{Eq.6}$$

In this study the SMES system used as first-order transfer function.

$$G_{SMES} = \frac{K_{SMES}}{1+T_{SMES}S} \quad \text{Eq.7}$$

where gain KSMES=0.98 , time constant TSMES= 0.03s

BES model

Battery energy storage is a device that converts chemically produced energy from renewable sources such as solar and wind into electrical energy, which is then stored in batteries for later use. As the globe progresses toward a more sustainable energy future, this technology is becoming increasingly crucial. Battery energy storage can assist in reducing the demand for traditional power plants, lowering emissions, and providing backup power during outages. It can also store extra energy generated by renewable resources for subsequent use when demand is higher. In this study, which will employ quick response types of BES devices, a first-order equation will be employed to represent the BES [5,7].

$$G_{BES} = \frac{K_{BES}}{1+T_{BES}S} \quad \text{Eq.8}$$

where gain KBES = 1.8 , time constant TBES= 0

4. Mountain gazelle optimizer MGO

The mountain gazelle is a species of gazelle found on the Arabian Peninsula and its surrounding areas, with low density due to its resemblance to the Robinia tree. Its territories are divided into mother-offspring herds, young male herds, and solitary male territories. The struggle for control of their environment between neighboring males is less violent and more dramatic than the conflict between male gazelles for female ownership. Young males use their horns more in combat than older males or landowners. The mountain gazelle is a migratory mammal that frequently travels over 120 kilometers in search of food, with an average speed of 49 miles per hour [25].

The Mountain gazelle optimizer algorithm uses the dynamic in society and groups of mountain gazelles to build a mathematical representation for its operations. This model considers the four major parts of a mountain gazelle's life: territorial males on their own, maternity herds, bachelor male herds, and food migration

Male mountain gazelles establish isolated territories, fiercely defending them, often facing conflicts over female custody. Older males defend their territories, while younger males attempt to conquer them. The MGO agent-based optimization technique is depicted in Figure 3.

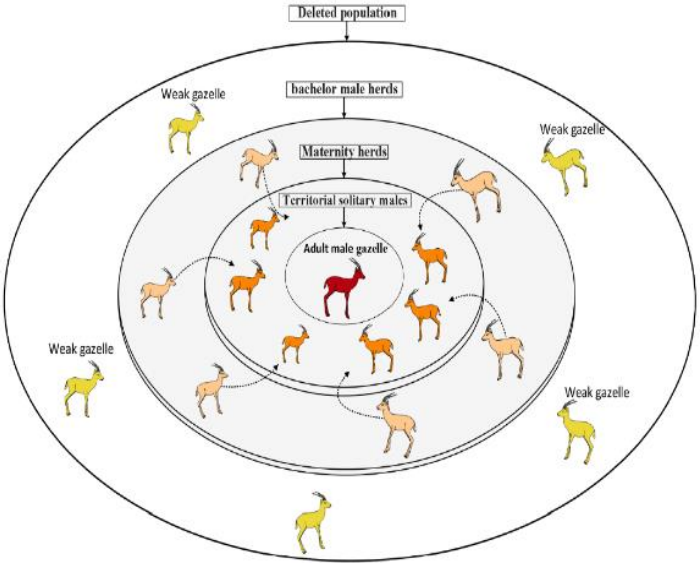

Fig. 3: Description of the improvement approach based on agents of MGO [25].

$$TSM = male_{gazelle} - |(r_{i1} \times BH - r_{i2} \times X(t)) \times F| \times Cofr \quad \text{Eq.9}$$

Where $male_{gazelle}$: a position vector that represents the ideal worldwide solution
r_{i1} and r_{i2} : random integers
BH: the coefficient vector of young male herd
Cofr: a coefficient vector that is randomly chosen and updated after each iteration.

$$BH = X_{ra} \times \lfloor r_1 \rfloor + Mpr \times \lceil r_2 \rceil, r_a = \{\lceil N/3 \rceil \dots N\} \quad \text{Eq.10}$$

X_{ra}: The random solution (young male) within the range of ra.
N : the total number of gazelles
Mpr: the typical number of search agents (N/3) that were randomly chosen.
r_1 chosen as random value also r_2.

$$F = N_1(D) \times \exp(2 - Iter \times (2 / Max_{Iter})) \quad \text{Eq.11}$$

$$Cofr = \begin{cases} (a + 1) + r_3, \\ a \times N_2(D), \\ r_4(D), \\ N_3(D) \times N_4(D) 2 \times \cos((r_4 \times 2) \times N_3(D)), \end{cases} \quad \text{Eq.12}$$

The amplitude (a) of Cofr is calculated by using this equation:

$$a = -1 + Iter \times (-1/Max_{Iter}) \quad \text{Eq.13}$$

where N1: selected randomly from the normal numbers.
Max_{Iter} : represents the total number of iterations, while Iter represents the current iteration.
r_3, r_4, and rand are arbitrary numbers from 0 to 1.
N_2, N_3, and N_4 : are arbitrary numbers that fall within the parameters and bounders of the problem.
r_4 : a random value that falls between 0 and 1 in the problem dimensions.
Cos : represents the cosine function.

Maternity herds are crucial for mountain gazelle life cycles as they provide a secure environment for females to give birth to robust males, who also contribute to reproduction through vying for females.

$$MH = (BH + Cof_{1,r}) + (r_{i3} \times malegazelle - r_{i4} \times X_{rand}) \times Cof_{1,r} \quad \text{Eq.14}$$

$Cof_{2,r}$ and $Cof_{3,r}$: coefficient vectors randomly chosen and independently calculated using eq.12.

X_{rand} : represents the gazelle's position along its vector that was randomly chosen from the entire population.

Male gazelles establish territories and attempt to control females after maturity, leading to confrontations and potentially violent behavior between young and older males.

$$BMH = (X(t) - D) + (r_{i5} \times male_{gazelle} - r_{i6} \times BH) \times Cofr \quad \text{Eq.15}$$

D: is The adult male calculated using the equation 22.

$$D = (|X(t)| + |male_{gazelle}|) \times (2 \times r_{i6} - 1) \quad \text{Eq.16}$$

Where r_6 is a random value from 0 to 1

Migration to Look for Food

Mountain gazelles are always on the move, moving large distances in search of food. They have exceptional agility and strength, allowing them to run quickly and jump high. This gazelle movement strategy is mathematically expressed in the equation below. The MGO flow chart is shown in Figure 8. An agent-based optimization strategy is used.

$$MSF = (ub - lb) \times r_7 + lb \quad \text{Eq.17}$$

Where ub: upper band

Lb: lower band

r_7 : an integer number amidst 0 and 1 that is randomly chosen

The algorithm starts by initializing a population of PID controller parameters. It then evaluates the performance of each set of parameters based on a fitness function, which could be a measure of the system's stability, response time, overshoot, and undershoot of the frequency deviation also power tie-line. The algorithm then iteratively updates the PID controller parameters based on the performance of the best parameters and some random factors, in a similar manner to how it updates the positions of the gazelles in the search space.

By doing so, the MGO algorithm can find the optimal PID controller parameters that yield the best performance for the load frequency control system. This makes the MGO algorithm a powerful tool for tuning PID controllers in load frequency control systems and other control systems. Figure 4 display the mountain gazelle optimizer flow chart. While t represents current iteration, T maximum iteration, X represent gazelle, and Pop represent population number of gazelle.

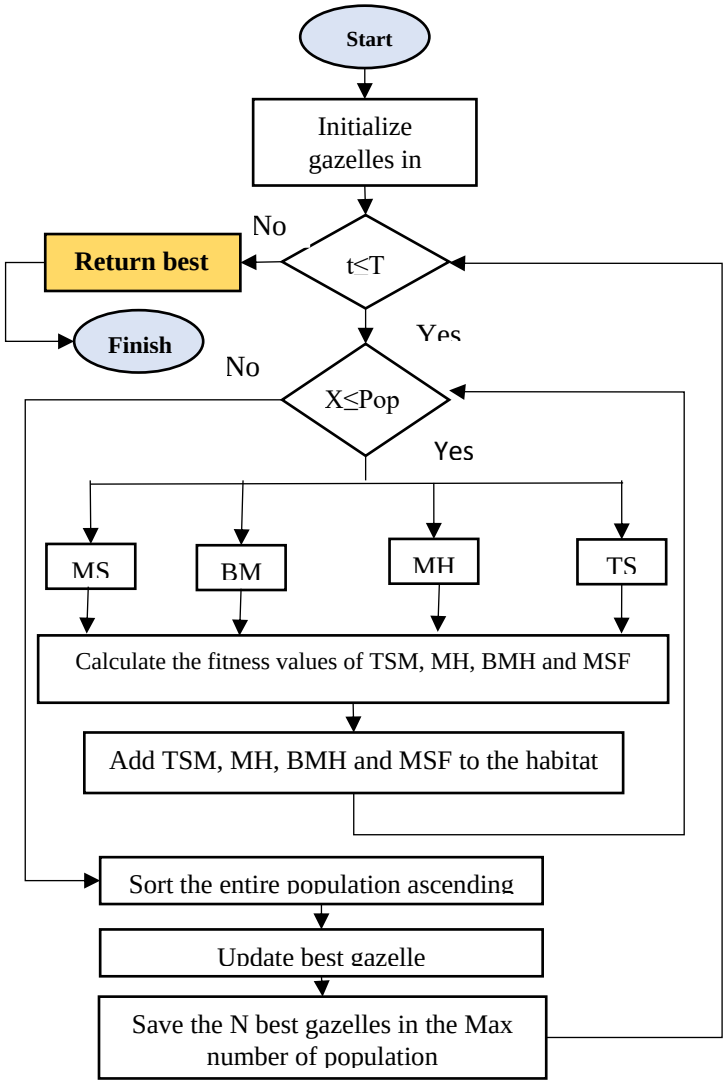

Fig. 4: flow chart of MGO[25]

ALGORITHM
PSEUDO-CODE OF MGO

Inputs: the population size N and the maximum number of iterations T
Outputs: gazelle's location and fitness potential
Create a random population using $X(i=1, 1,...,N)$
Calculate gazelle's fitness levels
While the stopping condition is not met
For each gazelle (Xi)
Calculate TSM using eq. (9)
Calculate MH using eq. (14)
Calculate BMH using eq. (15)
Calculate MSF using eq. (17)
Calculate the fitness values of TSM, MH, BMH and MSF, then add them To the habitat
End for
Sort the entire population in ascending order
Update $Best_{gazelle}$
Save the $Best_{gazelle}$ in the maximum number of populations
End while
Return $X_{Best\ gazelle}$

Fig 5: Pseudo-code of MGO [25]

5. Results and discussions

This study will use a three-area non-reheat system with and without storage energy to improve system stability, reduce frequency deviation, and keep tie-line power within limits. Two optimization techniques were used: the harmony search algorithm and the mountain gazelle optimizer. The optimization techniques will find the best parameters to enhance the system's stability. The storage energy will be inserted into the system to study its impact on frequency control. Figure 6 shows the change in load profile in each area. Authors in reference [27] uses two changes in load at area one (10%) and second zero, and 10% in area three at second 15. This scenario is modified in this study by adding another 10% change in load in area two at second 10, and changing the change time in area three to second 20.

Table 2 shows the best parameters that result from AI techniques with and without storage energy. Figure 7 shows the convergence curve for the proposed optimization algorithms MGO and HAS with and without energy storage.

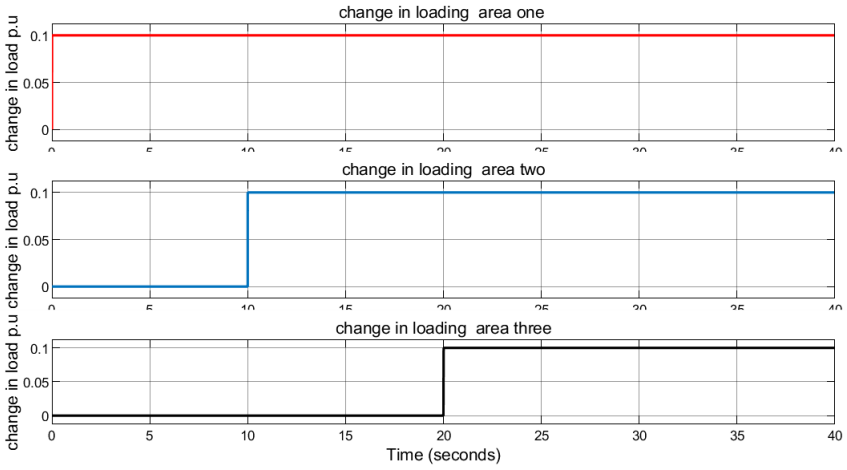

Fig 6: Change in loads in each area for a three-area system with and without storage energy

Table 2: PID controller parameters with& without storage energy

Technique	Controller	Area	K_p	K_i	K_d	N
HAS with energy ITAE= 0.0566	System controller	1	172.963	80.073	45.545	801.51
		2	194.197	96.247	3.354	238.508
		3	153.658	75.021	47.324	862.78
	Energy storage controller	1	79.641	93.736	3.311	697.04
		2	61.479	91.178	5.733	489.323
		3	99.789	95.045	19.921	1772.579
HAS ITAE= 0.07662	System controller	1	128.303	225.649	35.094	1302.143
		2	169.714	218.023	59.834	1833.223
		3	180.834	227.534	66.713	1834.131
MGO with RES ITAE= 0.0538	System controller	1	300	250	70	2000
		2	300	250	70	2000
		3	300	250	70	2000
	Energy storage controller	1	100	100	2	2000
		2	100	100	2	2000
		3	100	100	2	2000
MGO ITAE = 0.0767	System controller	1	293.097	245.767	69.551	1995.017
		2	291.058	243.903	47.667	1986.31
		3	299.782	248.985	62.847	1996.439

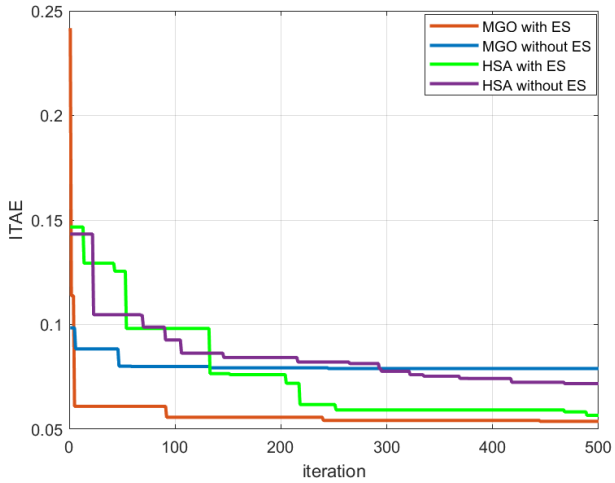

Fig 7: Convergence curve for the proposed methods to obtain parameters of system with and without storage energy

Figure 6 illustrates the load variations of 0.1 pu that occur in areas one, two, and three at 0, 10, and 20 seconds, respectively. Figure 7 depicts the convergence curve for iteration with ITAE for the proposed approaches to obtain system parameters with and without energy storage. The proposed methods include MGO with ES, MGO without ES, HAS with ES, and HAS without ES. The ITAE is used to evaluate the proposed methods performance. According to the results, MGO with ES achieves the lowest ITAE of 0.0538, and HAS with ES comes in second with an ITAE of 0.0566. MGO without ES and HAS without ES have the highest ITAE values, indicating that using ES improves the performance of the methods.

According to Figures 8-10, which show the frequency deviation in areas one, two, and three, MGO with ES proposed the best performance based on settling time, minimum overshoot, and undershoot. HAS with ES also exhibited good behavior compared to other techniques without energy storage. The performance of MGO without ES and HSA without ES was poor, as they exhibited high oscillations, overshoots, and undershoots in both frequency deviation and tie-line power. Table 3 summarizes and explains the results shown in Figures 8 to 10. Where include ΔPL change in load in each area. Sec which presents the time of change in load. Max overshoot and max undershoot for the frequency deviation in each area. As shown in Figures 8-10, the MGO with ES had the shortest average settling time of 2.366 seconds and no oscillation, unlike the MGO and HAS without ES. The HAS with ES also performed well, similar to the MGO with ES. The MGO with ES had the lowest overshoots and undershoots among the techniques. The maximum overshoot of 1.8×10^{-4} occurred in area two when a 10% load change was added in area three. The maximum undershoot of 1.7×10^{-3} also happened in area two due to the same load change. For HAS with ES the maximum overshoot of 2.5×10^{-4} occurred in area two when a 10% load change was added in area three. The maximum undershoot of 0.8×10^{-3} also happened in area two due to the same load change. HSA with energy storage, the average settling time was 2.777 seconds.

Figure 11 illustrates the change in power tie-line between areas for each technique. It is evident that MGO with energy storage has less oscillations than others, as it has the lowest change in power tie-line between areas and no oscillation. The peak power transfer from one area to another using MGO with ES was 1.85×10^{-4} p.u at second 1.5 and second 21.5. Moreover, any disturbance could be cleared in 7 seconds. HAS with ES also performed well in terms of tie-line power, with a maximum power transfer of 4×10^{-4} p.u at second 22. Any disturbance could be cleared in 10 seconds using this technique. HAS and MGO without energy storage had poor performance, with high oscillations in tie-line power.

Table 3: dynamic response of area one, two and three for different controllers

c Technique	Area	ΔPL	sec	Max overshoot	Max undershoots	S.T	Technique	Area	ΔPL	sec	Max overshoot	Max undershoots	S.T
MGO with ES	1	0.1	0	**0**	1.3e-3	**0.6**	HAS with ES	1	0.1	0	0	**1.2e-3**	0.7
	2	-	0	**0.8e-4**	**2.3e-4**	**3**		2	-	0	1e-4	2.3e-4	4
	3	-	0	**0.1e-4**	**2.3e-4**	**3**		3	-	0	0.5e-4	2.5e-4	3.3
	1	-	10	**0**	**2e-4**	**2**		1	-	10	0	2.4e-4	2
	2	0.1	10	**0**	**1e-5**	**0.8**		2	0.1	10	0	0.8e-3	1
	3	-	10	**0.5e-4**	**1.8e-4**	**4**		3	-	10	0.7e-4	2e-4	4
	1	-	20	**0.4e-4**	**1.2e-4**	**3.5**		1	-	20	1e-4	1.8e-4	4
	2	-	20	1.8e-4	**1.5e-4**	**3.4**		2	-	20	2.5e-4	2.5e-4	4
	3	0.1	20	**0**	1.7e-3	**1**		3	0.1	20	0	**0.8e-3**	2
MGO without ES	1	0.1	0	6.5e-3	11e-3	1.4	HAS without ES	1	0.1	0	5.2e-3	7.5e-3	1.4
	2	-	0	4.5e-4	2.5e-4	2.8		2	-	0	6.8e-4	6.4e-4	3
	3	-	0	4e-4	13e-4	4		3	-	0	2.5e-4	13e-4	3
	1	-	10	1.8e-4	7e-4	2.3		1	-	10	1e-4	10e-4	2.4
	2	0.1	10	6.5e-3	9.6e-3	1.5		2	0.1	10	5.1e-3	8.5e-3	1
	3	-	10	14e-4	6e-4	3		3	-	10	5.1e-4	4.8e-4	3
	1	-	20	6e-4	3.3e-4	3		1	-	20	3.4e-4	4e-4	3
	2	-	20	2.5e-4	12e-4	3		2	-	20	**2.2e-4**	1e-4	3
	3	0.1	20	4.8e-3	8e-3	1		3	0.1	20	4.5e-3	7.8e-3	1

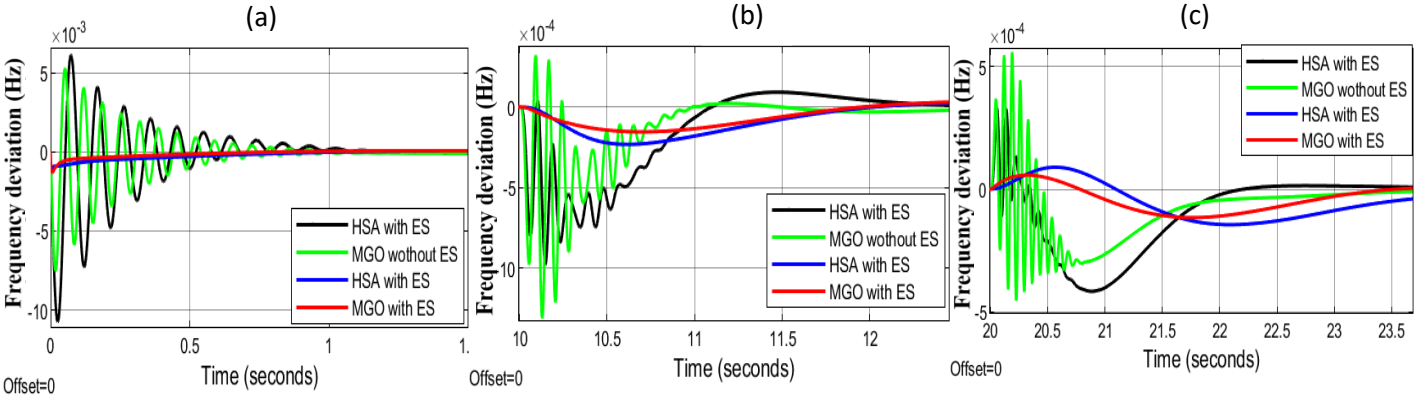

Fig 8: illustrates the frequency deviation of area one for a three-area non-reheat system with and without storage energy, as changes in load, based on the data presented in Figure 6; (a) time (s) from 0-1; (b) time (s) from 10-13; and (c) time (s) from 20-32.5

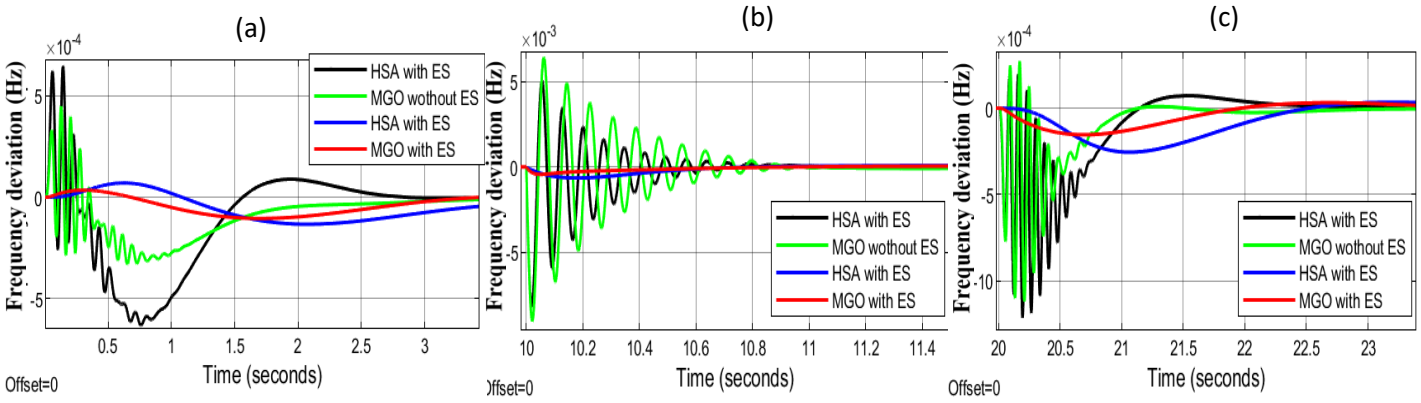

Fig 9: illustrates the frequency deviation of area two for a three-area non-reheat system with and without storage energy, as changes in load, based on the data presented in Figure 6; (a) time (s) from 0-1; (b) time (s) from 10-13; and (c) time (s) from 20-32.5

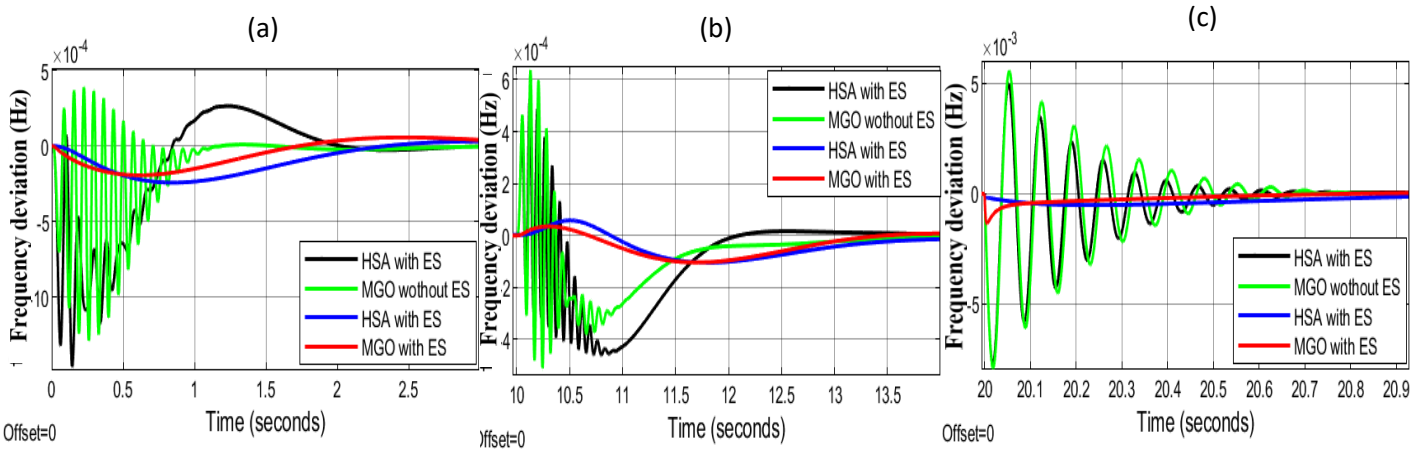

Fig 10: illustrates the frequency deviation of area three for a three-area non-reheat system with and without storage energy, as changes in load, based on the data presented in Figure 6; (a) time (s) from 0-1; (b) time (s) from 10-13; and (c) time (s) from 20-32.5

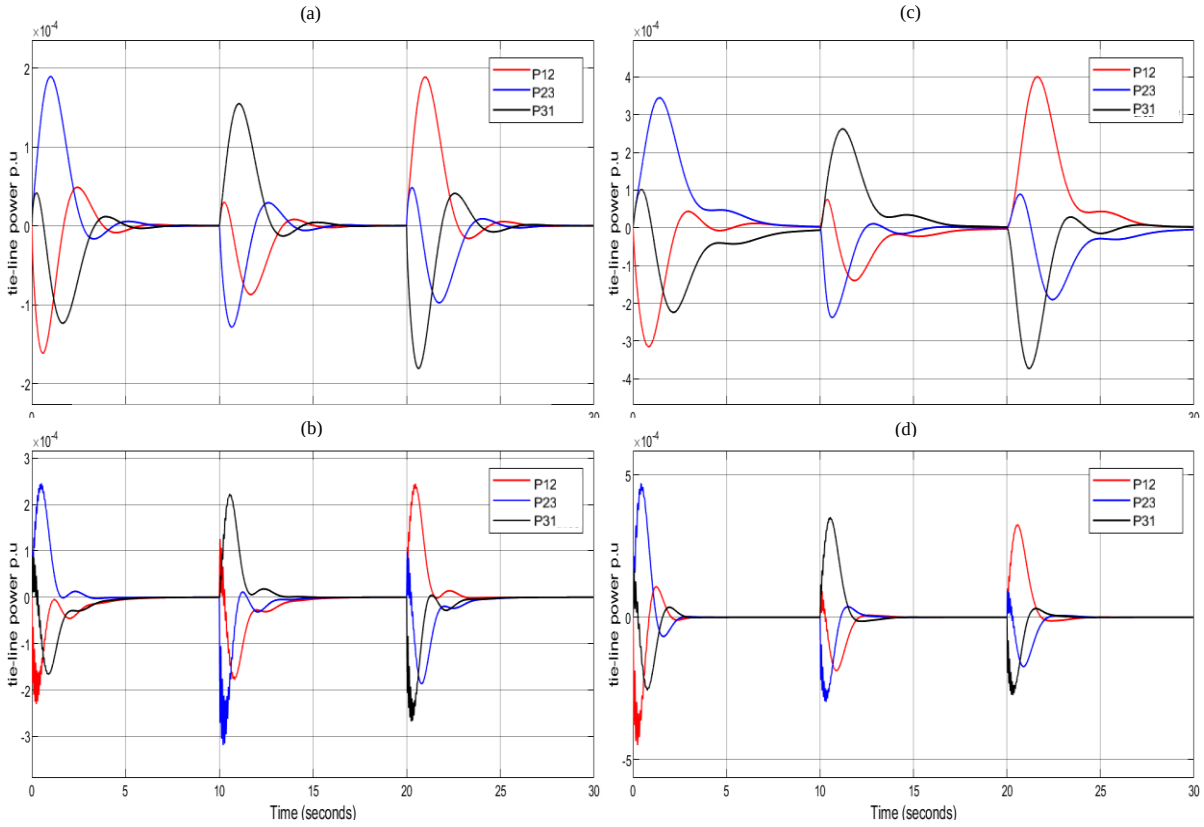

Fig 11: power tie-line for the proposed techniques during a sudden load change as appear in figure 6; (a) MGO with ES; (b): MGO without ES; (c): HAS with ES; (d): HAS without ES

6. Conclusion

This study proposed a method to enhance and maintain the load frequency control (LFC) using a proportional-integral-derivative (PID) controller with a derivative filter. The optimal parameters for the PID controller were obtained by two optimization techniques,

namely Mountain Gazelle Optimizer (MGO) and harmony search algorithm (HAS). A three-area non-reheat system with and without energy storage (ES) systems was evaluated under different load disturbances. The performance of the controllers was measured by frequency deviation, overshoot and undershoot settling time, tie-line power, and oscillation. The MGO-based PIDF with ES was the most effective controller that achieved the best performance in all criteria, with the lowest ITAE of 0.0538 and the fastest average settling time of 2.366 seconds. The HAS-based PIDF with ES also performed well, with an ITAE of 0.0566 and an average settling time of 2.777 seconds. The MGO-based PIDF and HAS-based PIDF without ES were less effective than the controllers with ES. Thus, the ES enhanced the system's resilience to sudden load changes and improved its LFC performance. The study's limitations include its focus on a three-area non-reheat system, which may not be representative of more complex power systems. Future work should extend the method to multi-area systems with different generator types such as reheat turbine, photovoltaic, wind tuberin and etc. a combination of MGO and other metaheuristic tetchiness to improve the controller's performance.

ABBREVIATIONS

BES	Battery energy storage	$\mathbf{M_{pr}}$	typical number of search agents
BH	the coefficient vector of young male herd	**MSF**	Migration to Search for Food
BMH	Bachelor Male Herds	**MUS**	maximum undershoot
$\mathbf{C_{ofr}}$	coefficient vector	**MW**	Mega watt
D	load damping coefficient	**R**	speed regulation
HSA	Harmony Search Algorithm	**SMES**	Superconducting magnetic energy storage
ITAE	integral time absolute error	**ST**	settling time
Iter	Iterations	$\mathbf{T_{12}}$	the synchronizing torque coefficient
$\mathbf{K_d}$	Derivative gain	**TSM**	Territorial Solitary Males
$\mathbf{K_i}$	Integral gain	**ub**	Upper
$\mathbf{K_p}$	Proportional gain	$\mathbf{T_{psi}}$	Generator time constant
lb	lower bounds	$\mathbf{T_g}$	Governor time constant
LFC	Load frequency control	$\mathbf{T_t}$	Turbine time constant
Max	Maximum	ΔP_L	change in load
$\mathbf{Max_{Iter}}$	total number of iterations	Δf_i	Frequency deviation, *i*= number of area
MGO	Mountain Gazelle optimizer	ACE	Area control error
MH	Maternity Herds	β	bias factor
Min	Minimum	$\mathbf{P_{tie}}$	Power tie-line
MOS	maximum overshoot		

References

1. H. K. Shaker, H. E. Zoghby, M. E. Bahgat and A. M. Abdel-Ghany, "Advanced Control Techniques for an Interconnected Multi Area Power System for Load Frequency Control," 2019 21st International Middle East Power Systems Conference (MEPCON), Cairo, Egypt, 2019, pp. 710-715, doi: 10.1109/MEPCON47431.2019.9008158.
2. Ashraf.H, Shimaa M, Mountasser.M "LOAD FREQUENCY CONTROL USING OPTIMIZED CONTROL TECHNIQUES" Journal of Engineering Sciences Assiut University Faculty of Engineering Vol. 48, No. 6 November 2020 PP. 1119-1136

3. Jin, L., He, Y., Zhang, CK. et al. Equivalent input disturbance-based load frequency control for smart grid with air conditioning loads. Sci. China Inf. Sci. 65, 122205 (2022). https://doi.org/10.1007/s11432-020-3120-0
4. Su K, Li Y, Chen J and Duan W (2021) Optimization and H∞ Performance Analysis for Load Frequency Control of Power Systems With Time-Varying Delays. Front. Energy Res. 9:762480. doi: 10.3389/fenrg.2021.762480
5. Dekaraja, B, Saikia, LC. Impact of energy storage and flexible alternating current transmission devices in combined voltage and frequency regulation of multiarea multisource interconnected power system. Energy Storage. 2022; 4(3):e317. doi:10.1002/est2.317
6. Mokhtar, M.; Marei, M.I.; Sameh, M.A.; Attia, M.A. An Adaptive Load Frequency Control for Power Systems with Renewable Energy Sources. Energies 2022, 15, 573. https://doi.org/10.3390/en15020573
7. A. H. Yakout, H. Kotb, H. M. Hasanien and K. M. Aboras, "Optimal Fuzzy PIDF Load Frequency Controller for Hybrid Microgrid System Using Marine Predator Algorithm," in IEEE Access, vol. 9, pp. 54220-54232, 2021, doi: 10.1109/ACCESS.2021.3070076.
8. Lili Dong, Yao Zhang, Zhiqiang Gao, A robust decentralized load frequency controller for interconnected power systems, ISA Transactions, Volume 51, Issue 3, 2012, Pages 410-419, ISSN 0019-0578, https://doi.org/10.1016/j.isatra.2012.02.004.
9. Nour EL Yakine Kouba, Mohamed Menaa, Mourad Hasni and Mohamed Boudour (Laboratory of Electrical and Industrial Systems, Faculty of Electrical Engineering and Computing, University of Science and Technology Houari Boumediene, El Alia 16111, Bab Ezzouar, Algiers, Algeria DOI: 10.15676/ijeei.2017.9.3.1
10. Prakash, Nisha, N. Karuppiah, V. Kumar, R. Vishnu and Zainy Mohammed Yousuf. "Load Frequency Control of Three Area System using FOPID Controller." WSEAS Transactions on Computers archive 6 (2018)
11. Zeynelgil, H.L.; Demiroren, A.; Sengor, N.S. The application of ANN technique to automatic generation control for multi area system. Electr. Power Energy Syst. 2002, 24, 345–354.
12. M.M. Ismail, A.F. Bendary, Load Frequency Control for Multi Area Smart Grid based on Advanced Control Techniques, AlexandriaEng.J.(2018), https://doi.org/10.1016/j.aej.2018.11.004
13. Sukhwinder Singh Dhillona, Jagdeep Singh Latherb, Sanjay Marwahac, Multi area load frequency control using particle swarm optimization and fuzzy rules, in: 3rd International Conference on Recent Trends in Computing (ICRTC), 2015, pp. 460–472.
14. S. Priyadharshini, P. Vanitha, Four area interconnected system on load frequency control using firefly algorithm, Int. J. Adv. Res. Electric. Electron. Eng. 3 (1) (2014), ISSN_NO: 2321-4775.
15. Pappachen, A.; Peer Fathima, A. Load frequency control in deregulated power system integrated with SMES-TCPS combination using ANFIS controller. Int. J. Electr. Power Energy Syst. 2016, 82, 519–534.
16. Dash, P.; Saikia, L.C.; Sinha, N. Flower pollination algorithm optimized PI-PD cascade controller in automatic generation control of a multi-area power system. Int. J. Electr. Power Energy Syst. 2016, 82, 19–28.
17. Bahgaat, N.K.; El-Sayed, M.I.; Hassan, M.A.M.; Bendary, F.A. Load frequency control in power system via improving PID controller based on particle swarm optimization and ANFIS techniques. Int. J. Syst. Dyn. Appl. 2014, 3, 1–24.
18. Zhang, F.; Li, Q. Deep learning-based data forgery detection in automatic generation control. In Proceedings of the 2017 IEEE Conference on Communications and Network Security (CNS), Las Vegas, NV, USA, 9–11 October 2017; pp. 400–404.
19. H. Li, J. Wang, Z. Du, F. Zhao, H. Liang, and B. Zhou, "Frequency control framework of power system with high wind penetration considering demand response and energy storage," The Journal of Engineering, vol. 2017, pp. 1153-1158, 2017. (Article)

20. J.G. Ziegler, N.B. Nichols, Optimum settings for automatic controllers, Trans. ASME 64 (1942) 759–768. (Article)
21. M. Farahani, S. Ganjefar and M. Alizadeh, “PID controller adjustment using chaotic optimization algorithm for multi-area load frequency control,” IET Control Theory & Applications, vol. 6, pp. 1984-1992, September 2012. (Article)
22. K.J. _Astro¨ m, T. Ha¨ glund, Revisiting the Ziegler-Nichols step response method for PID control, J. Process Control 14 (2004) 635–650. (Article)
23. Abdulslam A. Aloukili, Tarek M. Nasser, Mohammed A. Mehanna. (2023). IMPROVING LOAD FREQUENCY CONTROL USING A PID CONTROLLER WITH A DERIVATIVE FILTER BASED ON ARTIFICIAL INTELLIGENCE. Retrieved from http://jsju.org/index.php/journal/article/view/1813
24. K.Jagatheesan and Dr.B.Anand ” Load frequency control of an interconnected three area reheat thermal power systems considering nonlinearity and boiler dynamics with conventional controller” Advances in Natural and Applied Sciences, 8(20) Special 2014, Pages: 16-24
25. Benyamin Abdollahzadeh, Farhad Soleimanian Gharehchopogh, Nima Khodadadi, Seyedali Mirjalili, Mountain Gazelle Optimizer: A new Nature-inspired Metaheuristic Algorithm for Global Optimization Problems, Advances in Engineering Software, Volume 174, 2022, 103282, ISSN 0965-9978, https://doi.org/10.1016/j.advengsoft.2022.103282.
26. X. Wang et al., "An Introduction to Harmony Search Optimization Method", Springer Briefs in Computational Intelligence, DOI 10.1007/978-3-319-08356-8_2, 2015 http://www.springer.com/978-3-319-08355-1
27. Kunya, A.B., Argin, M., Jibril, Y. et al. Improved model predictive load frequency control of interconnected power system with synchronized automatic generation control loops. Beni-Suef Univ J Basic Appl Sci 9, 47 (2020). https://doi.org/10.1186/s43088-020-00072-w